Journal of Applied Geophysics 118 (2015) 24–36

Contents lists available at ScienceDirect

Journal of Applied Geophysics

journal homepage: www.elsevier.com/locate/jappgeo

The environmental magnetic record of palaeoenvironmental variations during the past 3100 years: A possible solar influence?

K. Sandeep [a,*], R. Shankar [a], Anish K. Warrier [a,1], Z. Weijian [b], Lu Xuefeng [b]

[a] Department of Marine Geology, Mangalore University, Mangalagangotri, 574 199, India
[b] Xi'an AMS Center, Institute of Earth Environment, Xi'an, China

ARTICLE INFO

Article history:
Received 17 September 2014
Received in revised form 16 March 2015
Accepted 18 March 2015
Available online 24 March 2015

Keywords:
Rock magnetism
Magnetic susceptibility
Rainfall
Lake sediments
Total solar irradiance
Spectral analysis

ABSTRACT

Sediments from Pookot Lake (PK) in southern India have provided a record of local environmental changes and catchment processes during the past 3100 cal. years B.P. Variations in the rock magnetic parameters (χ_{lf}, χ_{fd}, χ_{ARM} and IRM's at different field strengths) of sediments from two AMS ^{14}C-dated cores reflect climate-induced changes in the catchment of Pookot Lake. Assuming that rainfall is most likely the dominant driving mechanism behind the rock magnetic variations of PK sediments, the environmental history of the site has been reconstructed. Rock magnetic parameters exhibit significant variations during the past 3100 years. The palaeoenvironmental history of the Pookot Lake region may be divided into three phases. During the first phase (~3100 to 2500 cal. years B.P.), catchment erosion and detrital influx were high, indicating a strong monsoon. The second phase, which lasted from 2500 to 1000 cal. years B.P., was characterised by low and steady rainfall, resulting in a low and uniform catchment erosion and detrital influx. Phase 2 was interspersed with brief intervals of strong monsoon and characterised by frequent drying up of the lake. During Phase 3 (~1000 cal. years B.P. to the present), catchment erosion was high, indicating a shift to strong monsoonal conditions. It appears that monsoonal rainfall in the region is influenced by solar activity, with periods of high total solar irradiance being characterised by high rainfall and vice versa; it was relatively low during the Little Ice Age and high during the Medieval Warm Period. The magnetic susceptibility (χ_{lf}) data exhibit a number of periodicities which might have a solar origin. The χ_{lf} record exhibits similarities with other continental and marine palaeoclimatic records from the region, indicating that regional trends in the monsoon during the Late Holocene are broadly similar.

1. Introduction

Rock magnetism (or environmental magnetism) deals with the study of the magnetic properties of a wide range of natural materials including soil, sediment, dust and peat (Oldfield, 1999). Rock magnetic measurements have the advantages of being rapid, inexpensive, sensitive and non-destructive (Walden, 1999a). They have successfully been applied to characterise dust particles and atmospheric pollution (Warrier et al., 2014a; Blaha et al., 2008), study heavy metal pollution in soils and sediments (Wang, 2013; Pozza et al., 2004), understand pedogenic processes (Maher et al., 2003; Sandeep et al., 2012), reconstruct palaeoclimatic and palaeoenvironmental conditions (Shankar et al., 2006; Geiss et al., 2003), estimate opaque and heavy mineral contents in beach placers (Shankar et al., 1996), quantify particulate pollution in rivers (Sandeep et al., 2011), unmix sediment sources (Shankar et al., 1994; Yu and Oldfield, 1989), and characterise archaeological samples (Bradak et al., 2009; Mighall et al., 2009). Rock magnetic techniques have also been employed to study lake sediments (Geiss et al., 2003, 2004; Peck et al., 2004; Foster et al., 2008; Shankar et al., 2006; Warrier et al., 2014b), which provide information on the concentration, grain size and mineralogy of magnetic minerals present. This information may be used to determine catchment processes in response to environmental/climatic changes. Hence, past environmental/climatic changes may be reconstructed based on the rock magnetic data for lacustrine sediment cores. In India, most studies on lake sediments are confined to western India, Rajasthan and the Himalaya (Saini et al., 2005; Prasad and Enzel, 2006; Juyal et al., 2009; Kotlia et al., 2000; Krishnamurthy et al., 1986; Kajale and Deotare, 1997; Srivastava et al., 2013). Only a limited number of rock magnetic studies have been carried out on lake sediments of southern India to decipher palaeoenvironmental conditions (Shankar et al., 2006). There are thousands of lakes in southern India, which remain largely unexplored. In this paper, we have investigated sediments from the Pookot Lake (PK), southwestern India using rock magnetic methods to determine catchment-related and environmental processes during the past 3100 years.

Variations in the magnetic properties of lake sediments are dependent upon a variety of processes either outside the lake (pedogenesis

* Corresponding author at: Department of Post-Graduate Studies and Research in Geology, Government College Kasaragod, Kerala 671123, India.
E-mail address: sandeepk01@gmail.com (K. Sandeep).
[1] Present address: National Centre for Antarctic and Ocean Research (NCAOR), Earth System Science Organisation (ESSO), Ministry of Earth Sciences, Government of India, Headland Sada, Vasco-da-Gama, Goa 403 804, India.

http://dx.doi.org/10.1016/j.jappgeo.2015.03.023
0926-9851/

and erosion in the catchment) or within it (biogenic and authigenic). Ferrimagnetic iron sulphide (greigite) may form in anoxic environments characterised by high organic matter content and rapid sedimentation (Snowball, 1991; Roberts and Turner, 1993; Jelinowska et al., 1997). Its occurrence is usually coupled with dissolution of magnetite (Snowball and Thompson, 1990; Roberts and Turner, 1993; Anderson and Rippey, 1988), which may alter the magnetic signature recorded in sediments. Bacterial and anthropogenic magnetite may also be present in lake sediments. When post-depositional processes, anthropogenic, biogenic/authigenic effects are absent or limited, a simple model of detrital magnetic minerals being derived from a lake catchment may be used to semi-quantify the detrital flux from the catchment, either by runoff or aeolian processes (Dearing et al., 1981; Oldfield, 1991).

The main objectives of this investigation are to explore the (a) palaeoenvironmental changes of the Pookot Lake area during the Late Holocene, (b) presence of any periodicities in the sedimentary magnetic record, (c) influence of total solar irradiance on monsoon, and (d) regional trends in environmental changes by comparing them with other palaeoclimatic records from the region.

2. Materials and methods

2.1. Study area

Pookot Lake (PK) is a closed, natural lake situated at an altitude of 775 m in the *Sahyadri* (the Western Ghat) near Vythiri in Wayanad

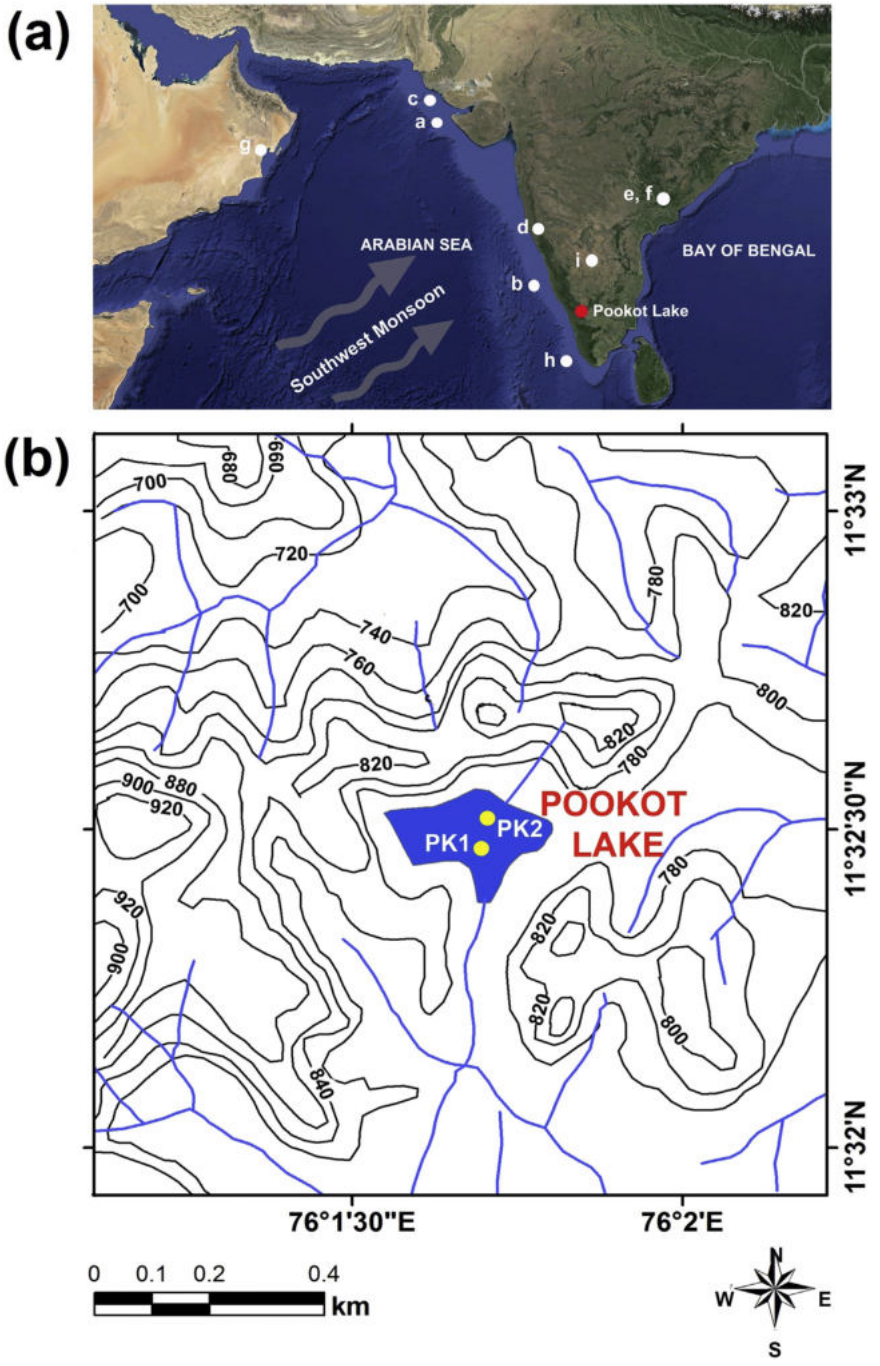

Fig. 1. (a) Satellite imagery showing the location of Pookot Lake in southwestern India and other palaeoarchives that are referred to in the text. (b) Location map showing the topography of the Pookot Lake and its surrounding area. Topographic contours are in metres. The locations of cores PK1 and PK2 are shown.

district, Kerala (11°32′30″N; 76°1′38″E; Fig. 1). It covers an area of 0.085 km^2 and has a maximum water depth of 6.5 m. The area surrounding the lake is covered by evergreen forest, and is in its natural setting. The area is pristine and without human perturbations. Its catchment is small (~0.74 km^2). Therefore, the magnetic (and other) properties of PK sediments must be a reflection of natural processes only and be correlatable with the changes in the PK catchment.

The main rock types of the PK catchment are hornblende–biotite gneiss and charnockite of the Late Archaeozoic Era (Geological and Mineral Map of Kerala, 1995; Soman, 1997). The main soil type is ferruginous forest loamy soil, which is shallow and immature that occurs under a canopy of vegetation mantling the gneissic/granulitic parent rocks in various stages of chemical weathering. It is dark reddish brown to black (Kerala Forest Department, 1986). The vegetation of the area falls in the category of western tropical wet evergreen forests of low elevation (Bonnefille et al., 1999).

The climate is generally moist with an average rainfall of 4200 mm per year (India Meteorological Department, 2008). The relative humidity is on the average between 65 and 80%. It is the highest during the southwest monsoon (95%). The temperature range is around 21–38 °C. Westerly winds blow across the area during the southwest monsoon (Kerala Forest Department, 1986; Chandran, 2003).

2.2. Sampling

Two undisturbed sediment cores (PK1 and PK2) from the Pookot Lake were collected in November 2007 by pushing PVC pipes (diameter: 1.5 in.) into the sediment. The lengths of the cores obtained are 2.4 m and 2.2 m (PK1 and PK2). In order to obtain high-resolution data, core PK1 was sub-sampled at 0.5 cm interval (n = 441) and core PK2 at 1 cm interval (n = 251). The sub-samples, packed in polythene covers, were stored in deep-freeze.

2.3. Chronology

Carbon-14 dating by accelerator mass spectrometry was carried out on the organic matter content of bulk sediment samples from selected depths. The details of the dates spanning the past 3100 years are given in Table 1. The ^{14}C ages were calibrated using the code clam (Blaauw, 2010), which runs on open source software 'R' (R Development Core Team, 2010) and uses IntCal09.14C calibration curve (Reimer et al., 2009). An age-depth model was constructed (Fig. 2) and age calculated for every depth (0.5 cm for PK1 and 1 cm for PK2) using a linear interpolation model. The R code of clam calculates the confidence intervals for undated levels from the calibrated age distribution (at 95% interval) of every dated depth and the age-model is drawn through these models and the calibrated age calculated (Blaauw, 2010) for every depth (0.5 cm for PK1 and 1 cm for PK2). The software obtains many calendar age estimates for every depth through repeated sampling (1000 times) from which the best age-depth model is calculated using the weighted mean of all the sampled calendar ages (Blaauw, 2010). Sedimentation rate was calculated from the age-depth model.

2.4. Rock magnetic measurements

Standard techniques were used for sample preparation (Walden, 1999a). Sediment samples were dried in a hot air oven at 35 °C and gently disaggregated using an agate mortar and a pestle. They were filled in polythene covers and tightly packed in 8-cc non-magnetic plastic bottles. Where insufficient quantity of sample was available, care was taken to position the sample in the centre of the plastic bottle. A range of magnetic parameters (χ_{lf}, χ_{fd}, χ_{ARM} and IRM's at different field strengths) was determined on the samples using standard methods (Dearing, 1999; Walden, 1999b; Thompson and Oldfield, 1986). Magnetic susceptibility at low (0.47 kHz; χ_{lf}) and high (4.7 kHz; χ_{hf}) frequencies was determined on a Bartington Susceptibility Meter (Model MS2B) with a dual-frequency sensor. Frequency-dependent susceptibility (χ_{fd} and χ_{fd} %) was calculated from the difference between the low- and high-frequency susceptibility values (Dearing, 1999).

Anhysteretic Remanent Magnetisation (ARM) was induced in the samples using a Molspin AF demagnetiser (with an ARM attachment) set with a peak alternating field (AF) of 100 mT and a DC biasing field of 0.04 mT. The ARM induced was measured on a Molspin spinner fluxgate magnetometer and expressed as susceptibility of ARM (χ_{ARM}) by dividing it by the size of the biasing field (0.04 mT = 31.84 A m^{-1}; Walden, 1999b).

Isothermal Remanent Magnetisation (IRM) was induced in the samples at different field strengths (20, 60, 100, 300, 500 and 1000 mT) using a Molspin pulse magnetiser. The isothermal remanence induced at 1 T field (the maximum field attainable in the Environmental Magnetism Laboratory at Mangalore University) was considered as Saturation Isothermal Remanent Magnetisation (SIRM). The remanence acquired was measured using the Molspin spinner fluxgate magnetometer. Inter-parametric ratios like S-ratio, χ_{ARM}/χ_{lf}, χ_{ARM}/SIRM and SIRM/χ_{lf} were calculated to determine the magnetic mineralogy and grain size.

Table 2 gives the details of the magnetic parameters and inter-parametric ratios studied, their units, interpretation and the instruments used (after Thompson and Oldfield, 1986; Maher, 1988; Oldfield, 1991, 1994, 2007; Oldfield et al., 2010; Snowball, 1991; Snowball and Thompson, 1990; Dearing et al., 1997).

2.5. Spectral analysis

Spectral analysis of the time series of environmental magnetic parameters was carried out using the Fortran-based programme REDFIT 3.8 (Schulz and Mudelsee, 2002). The spectra were estimated using the Lomb–Scargle Fourier Transform for unevenly spaced data, the

Table 1
AMS ^{14}C dates obtained on the organic matter content of bulk sediment samples from Pookot Lake. The ^{14}C dates were calibrated using the code clam (Blaauw, 2010), which runs on the open source software R (R Development Core Team, 2010), and IntCal09.14C calibration curve (Reimer et al., 2009). Sample PKB3 (depth = 90–91 cm, ^{14}C age = 430 ± 20 years) of core PK2 was not considered for the age-depth model as its age is nearly the same as that of the adjoining sample PKB2 (depth = 52–53 cm, ^{14}C age = 420 ± 20 years).

Core ID	Sample no.	Xi'an Lab ID	Depth (cm)	δ^{13}C (‰)	^{14}C age (years)	Weighted mean of calibrated age (years)	Calibrated age (cal. years B.P.) 2-σ
PK1	PKA1	XA3591	44–45	−32.30 ± 0.28	125 ± 20	133.3	269–13
	PKA2	XA3567	108–109	−33.97 ± 0.27	399 ± 20	468.1	507–335
	PKA3	XA3568	153–154	−32.31 ± 0.39	698 ± 24	650.4	683–567
	PKA4	XA3570	194–194.5	−25.95 ± 0.27	2003 ± 28	1952.1	2033–1884
PK2	PKB2	XA2996	52–53	−30.11 ± 0.44	420 ± 20	492.07	514–464
	PKB3	XA2997	90–91	−30.41 ± 0.38	430 ± 20	Date not used in age-depth model	
	PKB4	XA2998	143–144	−31.31 ± 0.35	734 ± 19	676.8	691–663
	PKB5	XA2999	193–194	−23.32 ± 0.37	1630 ± 22	1515.4	1595–1418
	PKB6	XA3000	214–215	−18.11 ± 0.45	2641 ± 21	2758.1	2777–2743
	PKB7	XA3001	235–236	−17.43 ± 0.80	2891 ± 26	3026.37	3142–2946

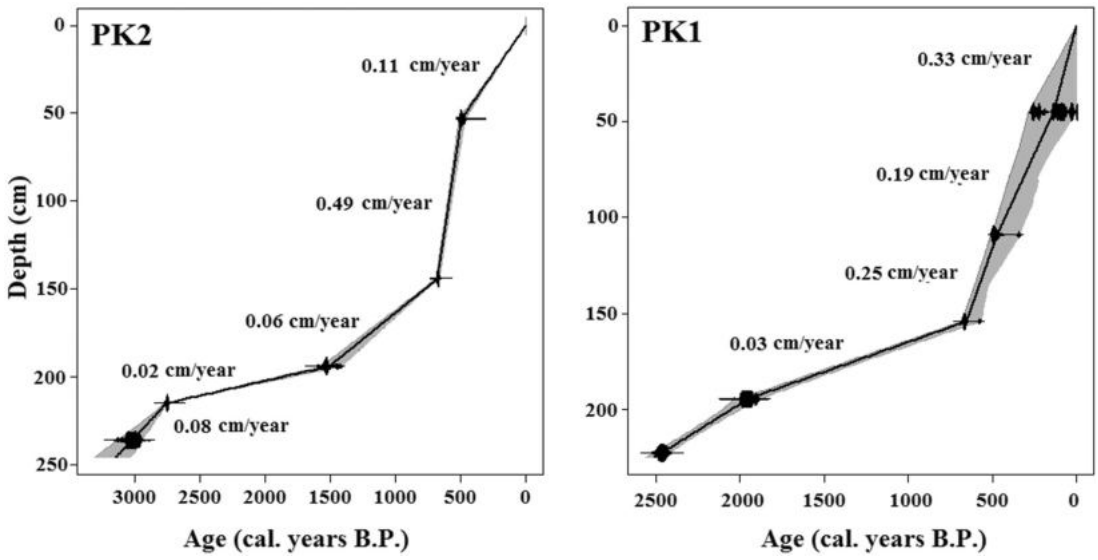

Fig. 2. Age-depth model for sediment cores PK1 and PK2. The age-depth model was constructed by linear interpolation model using the weighted mean of probability distribution of calibrated ^{14}C ages by R code of clam (Blaauw, 2010). The sedimentation rate is given for each interval. The 2σ probability range of each calibrated age is shown in black and that of interpolated ages in grey. The black line is the best age-depth model drawn through the weighted means of all the calendar ages.

Welch overlapped-segment-averaging procedure (four segments with 50% overlap) and linear detrending for each segment. The univariate spectra were bias-corrected using 1000 Monte-Carlo simulations (Schulz and Mudelsee, 2002). The oversampling factor (OFAC) was set at 4.0 and the maximum frequency to analyse (HIFAC) set to Nyquist frequency (1.0). The cross spectral and phase analysis were carried out using the software SPECTRUM 2.2 (Schulz and Stattegger, 1997).

3. Results and discussion

3.1. Chronology

The chronology of the two sediment cores is provided by 10 accelerator mass spectrometric (AMS) ^{14}C dates (four for core PK1 and six for core PK2). The calibrated age range at 95% confidence interval (2-σ)

Table 2
Magnetic measurements, their interpretation and instrumentation used in this study.
After Thompson and Oldfield (1986), Maher (1988), Oldfield (1991, 1994, 2007), Dearing et al. (1997), Snowball and Thompson (1990), Snowball (1991) and Oldfield et al. (2010).

Magnetic measurements and their units	Instruments used	Interpretation of rock magnetic parameters	Climatic interpretation
Low- and high-frequency magnetic susceptibility χ_{lf} and χ_{hf} (10^{-8} m^3 kg^{-1})	Bartington susceptibility metre with a dual-frequency sensor	Proportional to the concentration of magnetic minerals	A higher χ_{lf} value indicates a higher detrital influx (high rainfall) from the catchment and vice versa.
Frequency-dependent magnetic susceptibility χ_{fd} (10^{-8} m^3 kg^{-1}) $=\chi_{lf} - \chi_{hf}$	Bartington susceptibility metre with a dual-frequency sensor	Proportional to the concentration of superparamagnetic grains	A higher χ_{fd} value indicates a higher influx of pedogenic magnetite (=high rainfall) from the catchment to the lake-bed and vice versa.
Susceptibility of Anhysteretic Remanent Magnetization (ARM) χ_{ARM} (10^{-5} m^3 kg^{-1})	Molspin AF-demagnetiser with ARM attachment and fluxgate magnetometer	Proportional to the concentration of magnetic minerals of stable single domain size range	A higher χ_{ARM} value indicates a higher influx of pedogenic magnetite (=high rainfall) from the catchment to the lake-bed and vice versa.
Isothermal Remanent Magnetisation and Saturation Isothermal Remanent Magnetisation (IRM and SIRM) (10^{-5} A m^2 kg^{-1})	Molspin pulse magnetizer and fluxgate magnetometer	Proportional to the concentration of remanence-carrying magnetic minerals	Higher IRM and SIRM values indicate a higher detrital influx (high rainfall) from the catchment and vice versa.
'Hard' Isothermal Remanent Magnetisation HIRM = SIRM–$IRM_{300\ mT}$ (10^{-5} A m^2 kg^{-1})		Proportional to the concentration of magnetically 'hard' minerals like haematite and goethite	A higher HIRM value indicates a higher influx of haematite/goethite to the lake-bed. Higher haematite content indicates warm and oxidizing conditions.
χ_{ARM}/χ_{lf} χ_{ARM}/χ_{fd}		Indicative of magnetic grain size. A higher ratio indicates a finer grain size (fine SSD) and vice versa.	Higher ratio values indicate a higher influx of fine magnetic grains to the lake, and hence a higher rainfall. Values of $\chi_{ARM}/\chi_{lf} > 40$ and $\chi_{ARM}/\chi_{fd} > 1000$ are indicative of bacterial magnetite.
χ_{ARM}/SIRM		A higher ratio value indicates a finer magnetic grain size and vice versa.	A higher ratio value indicates a higher influx of fine magnetic grains to the lake, and hence higher rainfall. Very low ratio values indicate a coarser magnetic grain size, indicative of anthropogenic sources.
SIRM/χ_{lf}		High ratio values (~70×10^3 A m^{-1}) are indicative of greigite.	Higher ratio value indicates reducing conditions.
S-ratio = $IRM_{300\ mT}$/SIRM		Indicative of the relative proportion of ferrimagnetic and anti-ferromagnetic minerals (high ratio = A relatively higher proportion of magnetite).	Higher ratio indicative of higher influx of softer magnetic minerals like magnetite/maghemite into the lake and lower ratio indicative of higher influx of haematite/goethite to the lake bed. Higher haematite indicates warm and oxidizing conditions.

and the weighted mean of the calibrated age range are given in Table 1. Sample PKB3 (depth = 90–91 cm, ^{14}C age = 430 ± 20 years) of core PK2 was not considered for the age-depth model as its age is nearly the same as that of the adjoining sample PKB2 (depth = 52–53 cm, ^{14}C age = 420 ± 20 years). The underlying assumptions in this model are that the sedimentation rate was uniform between successive ^{14}C-dated layers, the core-top has a zero age, there was no loss/compression of sediments and no bioturbation.

The maximum ^{14}C age obtained for the two cores is 2891 ± 26 years. In core PK2, no dates are available beyond 236 cm depth down to the core-bottom (246 cm). Hence, ages for sediment layers in this segment of the core were assigned by extrapolation though this may have led to uncertainties. Similarly, core PK1 does not have any dates beyond 194.5 cm depth. But ages were assigned to sediment layers in this segment of the core by correlating the peaks in magnetic susceptibility values of PK1 and PK2. Fig. 3 depicts the χ_{lf} vs. calibrated age for cores PK1 and PK2. In spite of differences in the magnitudes of χ_{lf} values, there is a good overall correlation between the two cores. Corresponding peaks in χ_{lf} are discernible in both the cores and may be used for correlation. Correlatable peaks are shown by broken lines in Fig. 3. A prominent peak in χ_{lf} (148.2×10^{-8} m^3 kg^{-1}) is documented in PK1 at a depth of 222.5 cm, which may be correlated with a peak in PK2 at 2462.2 cal. years B.P. with a χ_{lf} value of 89.8×10^{-8} m^3 kg^{-1}. Hence, the age-depth model for PK1 assumed an age of 2462.2 cal. years B.P. for 222.5 cm depth. Pookot Lake core-top samples were analysed for ^{210}Pb and ^{137}Cs activities to determine the modern sedimentation rate and thus an accurate chronology for the core-top. No significant ^{210}Pb and ^{137}Cs activities or peak was detected above the background level. This is probably because the sample quantity (3–4 g) was not enough even after combining 4–5 sub-samples from adjacent depths. This may be due to the possibility that a large fraction of these isotopes may have decayed, leaving only a small activity to be detected. Hence, an age of −57 cal. years B.P. was assigned to the core-top (i.e., 0 cm) as the core was collected in 2007 A.D.

The sedimentation rate is not uniform both within and between the two cores. It varies from 0.02 cm/year to as high as 0.49 cm/year. The average sedimentation rate is 0.175 cm/year for PK1 and 0.15 cm/year for PK2 (Fig. 2). Each 0.5 cm sub-sample of core PK1 represents 2.11 years up to 44 cm depth; however, it represents 2.62 years (44–108.5 cm), 2.03 years (108.5–153.5 cm), 16.07 years (154–194.5 cm) and 9.11 years (194.5–225 cm). Similarly, in core PK2, each 1 cm sub-sample represents 10.36 years up to 52 cm depth; however, it represents 2.03 years (52–143 cm), 16.77 years (143–193 cm), 59.17 years (193–214 cm) and 12.78 years (214–246 cm). This variation in sample resolution may be attributed to changes in the sedimentation rate.

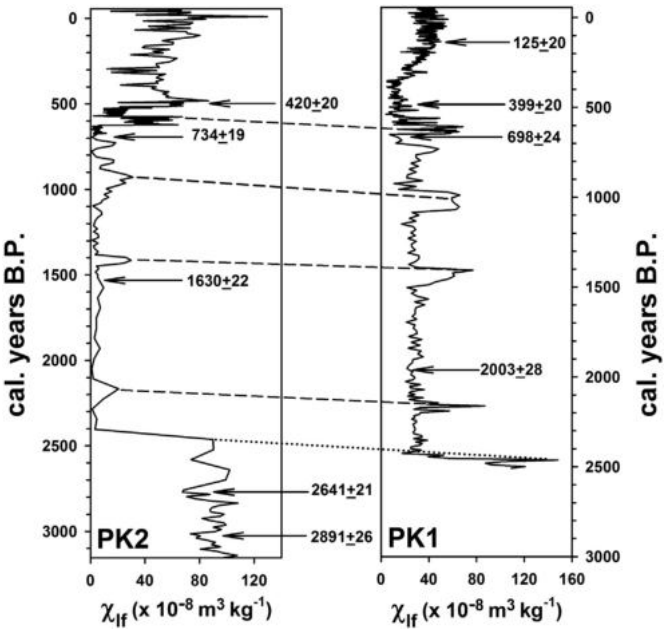

Fig. 3. Magnetic susceptibility vs. age diagrams for cores PK2 and PK1. Note: The two cores are correlatable; the corresponding peaks are joined using broken lines. The radiocarbon ages obtained are indicated with arrows pointing to sediment depths in the cores. The bottom most peak in PK1 (shown using dotted lines) has been assigned an age corresponding to that of a correlatable peak in PK2.

3.2. Source of magnetic minerals in the PK sediments

In order to appreciate the palaeoenvironmental significance of magnetic proxies, it is essential to determine their origin which is possible through the magnetic parameters. Down-core variations of rock magnetic parameters for cores PK1 and PK2 are displayed in Fig. 4. The SIRM/χ_{lf} ratio may be used to detect the presence of greigite in sediments. High SIRM/χ_{lf} values (~70×10^3 A m^{-1}) are indicative of greigite (Snowball and Thompson, 1990; Snowball, 1991; Oldfield et al., 2010). But Pookot Lake sediments exhibit values that are less than the one ascribed for greigite (Fig. 4a and b). Hence, the possibility of greigite contributing to the magnetic make up of Pookot Lake sediments is ruled out.

Magnetic minerals are also produced within a lake as a result of bacterial activity, notably of magnetotactic bacteria. Magnetite produced thus has stable single domain (SSD) grain size with grain diameter ranging from 0.02 to 0.1 μm (Oldfield et al., 2010). Hence, the relative importance of bacterial magnetite in sediments may be evaluated qualitatively by χ_{ARM} and interparametric ratios derived from it (Oldfield et al., 2010). When bacterial magnetite is present, χ_{ARM}/χ_{lf} and χ_{ARM}/χ_{fd} exhibit considerably high values, i.e., χ_{ARM}/χ_{lf} >40 and χ_{ARM}/χ_{fd} >1000 (Oldfield, 1994, 2007) and plot in a distinct envelope in the biplot of the two parameters. But Pookot Lake sediment samples exhibit values that are considerably lower than those prescribed for bacterial magnetite (Fig. 5). χ_{ARM}/SIRM has also been used to detect the presence of bacterial magnetite (Oldfield et al., 2010) with a value of $>200 \times 10^{-5}$ mA^{-1}. A majority of the Pookot Lake samples exhibit low values (Fig. 6a); a few do exhibit slightly higher values. But they are for individual samples scattered throughout the core (Figs. 4a, b and 6) and not being restricted to a particular depth range. This indicates that there is no sustained contribution from magnetotactic bacteria (Oldfield et al., 2010). A comparison of data for PK sediments and catchment soils indicates that χ_{ARM}/SIRM ratio values range from 51 to 207×10^{-5} mA^{-1} (average = 120×10^{-5} mA^{-1}) for catchment soils whereas those of sediment samples from both the cores range from 2 to 204.5×10^{-5} mA^{-1} (average = 128×10^{-5} mA^{-1}). However, values of concentration-dependent parameters, χ_{lf} and SIRM, are much higher for catchment soils when compared to sediments (Fig. 5b). This may be due to the diamagnetic effect of sand and organic matter in sediments (Oldfield et al., 2010). As the magnetic grain size of both the catchment soils and lake sediments are similar (Figs. 6a and 7), it is inferred that magnetic minerals are of detrital, but not bacterial, origin.

The magnetic properties of anthropogenic magnetic minerals differ from those of naturally produced magnetic minerals (Oldfield et al., 1985) in having a coarse magnetic grain size (MD and PSD; Warrier et al., 2014a; Shen et al., 2008; Gautam et al., 2004). Magnetic grain size may be determined semi-quantitatively using the bi-plot of χ_{ARM}/SIRM vs. χ_{fd} % (Dearing et al., 1997). A majority of the Pookot Lake sediment samples plot in the regions of coarse SSD to SSD/SP transition range (Fig. 7), indicating a fine magnetic grain size. This indicates that there is no anthropogenic contribution to the magnetic signal carried by Pookot Lake sediments, which have a coarse magnetic grain size. Moreover, the lake is situated well away from industries and pollution sources. At the present time, the lake is situated in a tropical evergreen forest that falls under the jurisdiction of the South Wayanad Forest Division. The catchment area of the lake is rather small and without much

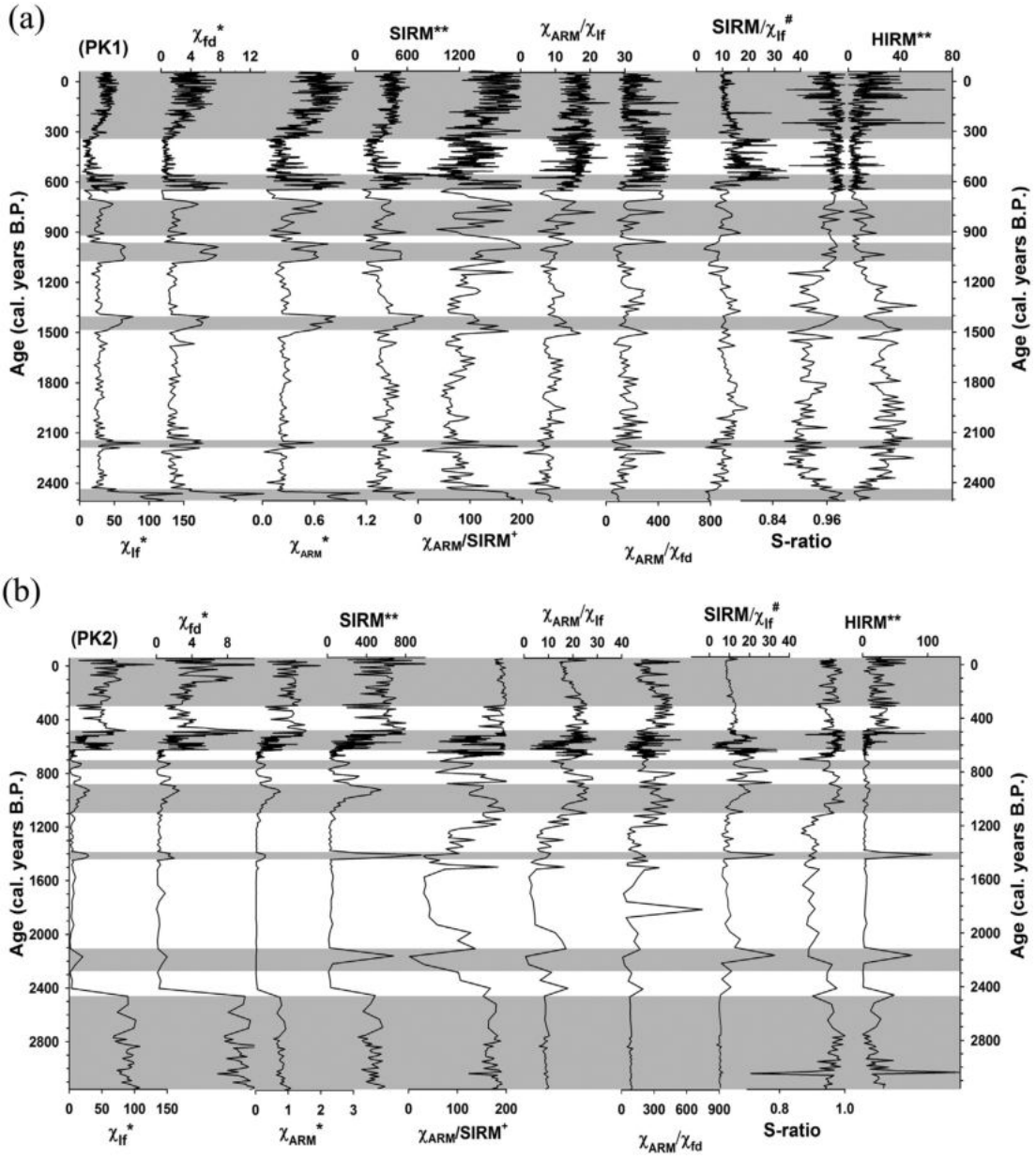

Fig. 4. Down-core variations of rock magnetic parameters for cores PK1 (a) and PK2 (b). Periods with high rainfall are shaded with grey. Note the almost similar trends of concentration-dependent parameters. Low-rainfall periods are characterised by magnetically fine grain size and vice versa. Magnetic mineralogy is predominantly "soft", but some periods are characterised by a slightly high proportion of magnetically "hard" minerals. (* $= \times 10^{-8}$ m^3 kg^{-1}; ** $= \times 10^{-5}$ A m^2 kg^{-1}; # $= \times 10^{-5}$ m A^{-1}).

human settlement. Hence, it is reasonable to assume that there may not have been anthropogenic activities during the past also. The historical lines of evidence suggest that there was no organised human settlement in the area surrounding the Pookot Lake till the 18th century. A microscopic examination of sediment samples from Pookot Lake did not reveal the presence of any charcoal pieces. This indicates the absence of fire-related activities due to human intervention. Soils affected by fire bear a distinct rock magnetic signature with low χ_{ARM}/χ_{lf} and χ_{ARM}/χ_{fd} values (Oldfield and Crowther, 2007). The samples from Pookot Lake region do not plot in the envelope of fire-affected samples (Fig. 5). Pollen analysis of Pookot Lake sediments (Bhattacharyya et al., under review) reveals the dominance of pollen of high land taxa, mangroves and Poaceae. Pollen grains from agricultural or cultivated plants are not detected. These data indicate that there were no agricultural activities in the regions surrounding the Pookot Lake, ruling out any human intervention influencing the detrital influx to the lake.

Dissolution of magnetic minerals has to be verified before using magnetic parameters as a climate/environment proxy. The absence of greigite and the negligible sulphur content in PK sediments indicate that reducing conditions necessary for iron oxide dissolution are absent. Hence, dissolution of magnetic minerals in PK sediments may be ruled out.

There is a proportion of SP grains in PK sediments as indicated by the high χ_{fd} % values (0.2 to 14%; average = 7.7%). The SP grains in PK sediments are derived from catchment soils. There is a high production of pedogenic magnetite (of SP grain size) in tropical soils as revealed by many studies (Sandeep et al., 2012; Ananthapadmanabha et al., 2014a, 2014b). This is confirmed by the χ_{fd} % values of catchment soils which vary from 1.7 to 12% (average = 8.8%). These values are in the same range as those of PK sediments.

The detrital influx may be related to changes in catchment erosion which, in turn, is related to rainfall. Hence, it may be argued that rainfall is the most likely driving mechanism behind the variations in the magnetic properties of lake sediments.

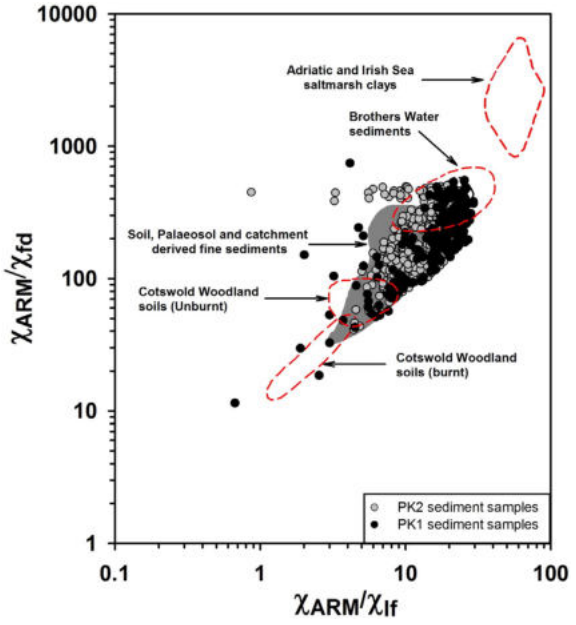

Fig. 5. Bi-plot of χ_{ARM}/χ_{lf} vs. χ_{ARM}/χ_{fd} (Oldfield, 1994; Oldfield and Crowther, 2007) for Pookot Lake sediment samples. Note: Most of the PK sediment samples plot in the envelope for soils, palaeosols and catchment-derived fine sediments.

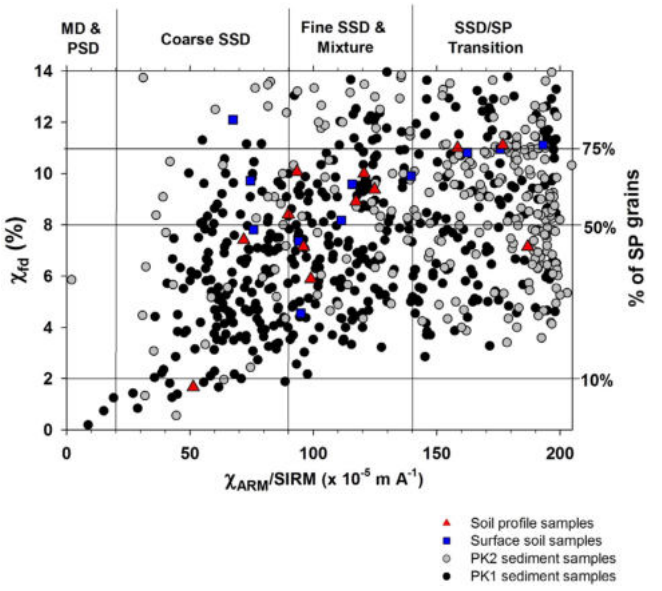

Fig. 7. Semi-quantitative magnetic granulometry plot of χ_{ARM}/SIRM vs. χ_{fd} % (after Dearing et al., 1997; Maher and Taylor, 1988) for Pookot Lake sediment samples and catchment soils (Sandeep et al., 2012). Note the large variations in the magnetic grain size of Pookot sediment samples.

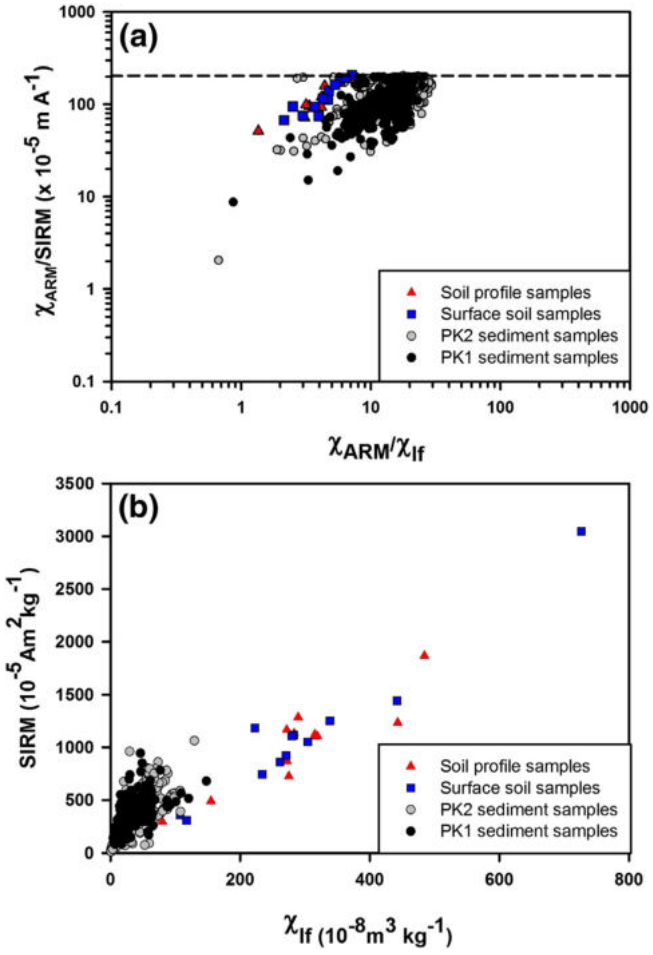

Fig. 6. Bi-plot of (a) χ_{ARM}/SIRM vs. χ_{ARM}/χ_{lf} (logarithmic scale) and (b) χ_{lf} vs. SIRM for Pookot Lake sediment and catchment soil (Sandeep et al., 2012) samples. Note: Most of the PK sediments and catchment soils exhibit χ_{ARM}/SIRM values of $<200 \times 10^{-5}$ m A^{-1}. The magnetic grain size of PK sediments is similar to that of catchment soils. However, the magnetic mineral concentration is relatively high in the latter.

3.3. Environmental magnetic record of Pookot Lake sediments

The trends exhibited by the concentration-dependent parameters – χ_{lf}, χ_{fd}, χ_{ARM} and SIRM – are almost similar (Fig. 4a and b). All of them are strongly correlated with χ_{lf}. As IRM values (at 20–500 mT field strength) also exhibit a trend similar to that of χ_{lf}, they were not plotted. The χ_{lf} curve closely matches that of χ_{fd}. The generally high χ_{fd} % values (average = 8% and maximum of 14%) indicate a significant contribution by magnetite/maghemite of SP size resulting from pedogenic processes (Maher and Thompson, 1992; Maher and Taylor, 1988).

The Pookot Lake sedimentary χ_{lf} record shows episodes of high and low detrital influx which, in turn, may be related to relatively high and low precipitation respectively (Fig. 4a and b). As most of the concentration-dependent magnetic parameters exhibit similar trends, variations in χ_{lf} only are discussed here. During the period ~3100 to 2400 cal. years B.P., χ_{lf} exhibits the highest values in the entire core. It decreases abruptly from 2400 cal. years B.P. and remains steady but low up to 1100 cal. years B.P. However, this period was interspersed with peaks of high χ_{lf}. About 1100 cal. years B.P. onwards, χ_{lf} values exhibit an overall increasing trend, but interspersed with periods of low χ_{lf}.

The χ_{ARM}/SIRM ratio has been used to identify the relative changes in the magnetic grain size of minerals above the SP/SD threshold (Thompson and Oldfield, 1986). The χ_{ARM}/SIRM ratio exhibits a strong correlation with χ_{lf} ($r = 0.50$). High values of χ_{ARM}/SIRM are indicative of a fine magnetic grain size and vice versa (Dearing et al., 1997). The ratio values indicate that during periods of high intensity of chemical weathering, the magnetic grain size was fine and vice versa. The χ_{ARM}/SIRM ratio values suggest a wide variation in the magnetic grain size of Pookot Lake sediments (Fig. 7). Samples from periods of low detrital influx are characterised by magnetically coarse grains whereas those of high detrital influx periods contain fine grains (Fig. 4a and b). The overall decrease/increase in magnetic grain size during high/low rainfall periods may be due to high/low production of fine grained pedogenic magnetic minerals due to high/low intensity of chemical weathering and pedogenesis in the catchment. It has been reported that magnetically coarse (MD) grains are converted into fine (SP and SSD) grains during pedogenesis in tropical regions (Ananthapadmanabha et al., 2014b, 2014). Rainfall is one of the important factors which control this process.

The magnetic mineralogy of Pookot Lake sediments is dominated by magnetically "soft" minerals as indicated by the high S-ratio values which range from 0.86 to 1. Although the range of variation in S-ratio values is small throughout the core, there are slight variations during the 2400–1000 cal. year B.P. period (average S-ratio value = 0.90) compared to the post-1000 cal. year B.P. period (average S-ratio value = 0.97; Fig. 4a and b). Water saturation alters the redox state of soils, leading to magnetite formation during periods of enhanced precipitation, but to haematite formation through oxidative processes (Maher and Thompson, 1995). Probably, the lake dried up frequently during this period, exposing the lake-bed and leading to the formation of haematite due to oxidation.

3.4. Magneto-climatic interpretation of Pookot Lake sedimentary record

The palaeoenvironmental history of the Pookot Lake region may be divided into three phases based on the rock magnetic properties of PK sediments.

Phase 1 (~3100–2500 cal. years B.P.): This period is characterised by very high detrital influx of to the lake resulting from intense catchment erosion. This is evident from the high values for concentration-dependent magnetic parameters (χ_{lf}, χ_{ARM} and SIRM). The high rainfall caused by intensified monsoon would have carried more magnetic mineral grains to the Pookot Lake. Hence, strong monsoonal conditions must have prevailed during this period.

Phase 2 (~2400–1000 cal. years B.P.): This period was characterised by very low detrital influx and catchment erosion as evident from the low values for concentration-dependent magnetic parameters. This indicates low rainfall during the period except a few brief spells of high rainfall. The lake would have dried up frequently during this period as evident from the presence of haematite. Towards the end of this period, rainfall exhibits an increasing trend.

Phase 3 (~1000 cal. years B.P. to the Present): Detrital influx to the lake exhibits wide variations during this period. Overall, it shows an increasing trend. Precipitation was overall high when compared to Phase 2. However, it was interspersed with a few low-precipitation intervals.

3.5. Relationship between magnetic susceptibility and total solar irradiance (TSI)

Fig. 8 presents the Pookot Lake sediment χ_{lf}, TSI data based on cosmogenic radioisotopes (Steinhilber et al., 2012), and TSI data based on sunspot numbers (Lean et al., 1995). A visual comparison of the curves shows that their broad trends are similar. During the Medieval Warm Period (MWP; 900–1400 AD) when TSI was high, χ_{lf} values generally exhibit an increasing trend, save for the two intervening periods of solar minima – the Wolf Minimum (1282–1342 AD) and the Oört Minimum (980–1120 AD) – for which conspicuous decreasing trends in χ_{lf} values are documented (Fig. 8a–c). The Wolf and Oört Minima are not aligned with the troughs in magnetic susceptibility and there is a slight offset. This may be attributed to the uncertainties in the age-depth model.

During the Maunder (1645–1715 AD) and the Spörer (1416–1534 AD) Minima, which bracket the Little Ice Age (LIA), TSI was lower by as much as 0.25% (Lean et al., 1995). These periods are characterised by low χ_{lf} values. There was a complete absence of sunspots (Fig. 8d) during the Maunder Minimum (Eddy, 1976). The Spörer Minimum had a much lower TSI compared to the Maunder Minimum. These characteristics are also mirrored in the χ_{lf} values, i.e., much lower during the Spörer Minimum and slightly higher during the Maunder Minimum. In fact, the χ_{lf} values during the Little Ice Age are significantly low compared to the rest of the core.

The Dalton Minimum (1790–1820 AD) was characterised by low values of TSI and sunspot number. However, a decrease in χ_{lf} values is not recorded for the same period, but slightly earlier (1750–1780 AD). Similarly, although a minimum in solar activity is documented around 1900 AD (1880–1900 AD), the corresponding low χ_{lf} values are documented slightly earlier (~1860–1880 AD). From 1900 AD to the Present, an overall increasing trend in TSI is apparent except for a slight decrease during 1940–1970 AD. But the χ_{lf} values do not increase correspondingly, the overall trend remaining steady.

Spectral analysis for the period −57 to 1100 cal. years B.P. of the original χ_{lf} data yielded periodicities of 469, 209–134, 14.3, 10, 8.5, 8.1 and 7.8 years (Fig. 9a). It is interesting to note that many periodicities recorded in the χ_{lf} time series of Pookot Lake sediments are similar to those documented in other palaeoclimatic records from the region and to the solar modulated tree ring $\Delta^{14}C$ record of Damon and Peristykh (2000) (Supplementary Table S1). In order to check whether these periodicities had a solar origin, cross spectral analysis of χ_{lf} was attempted with group sunspot number (Hoyt and Schatten, 1997) as well as with annual (Wolf) sunspot number data. The results showed a high coherency for several periodicities at 90% significance level (Fig. 10a and b). Periodicities with high coherency are 91, 37, 24.8, 12.8–11.9, 8.2 and 5.5 years for sunspot numbers. For group sunspot

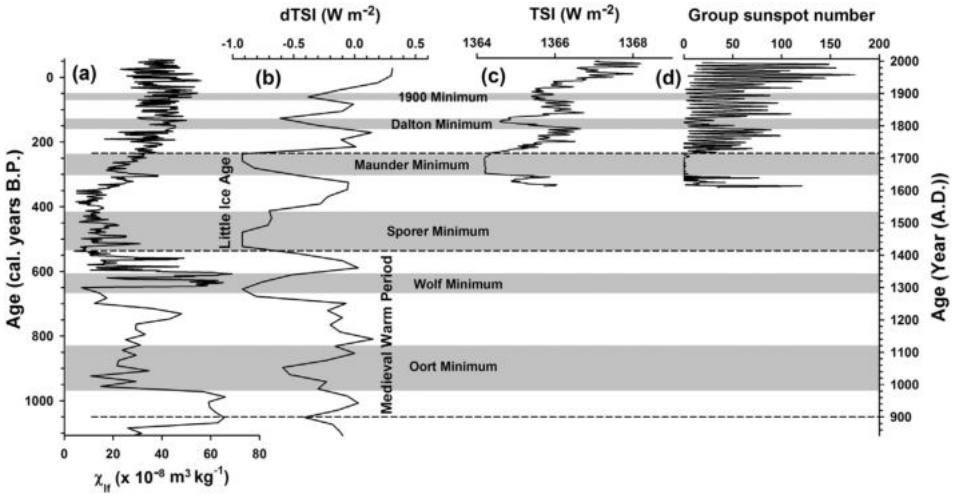

Fig. 8. Comparison of the Pookot Lake sediment magnetic susceptibility (χ_{lf}) of the past 1117 years (a) with: Reconstructed total solar irradiance (TSI) based on cosmogenic radioisotopes (Steinhilber et al., 2012; given as difference to the value of the PMOD composite during the solar cycle minimum (1365.57 W/m^2) of the year 1986 AD) (b), TSI reconstructed based on sunspot numbers (Lean et al., 1995) (c), and Group sunspot numbers (d). Note the similarities in the broad trends of χ_{lf} and TSI curves, with periods of high TSI being associated with high χ_{lf}.

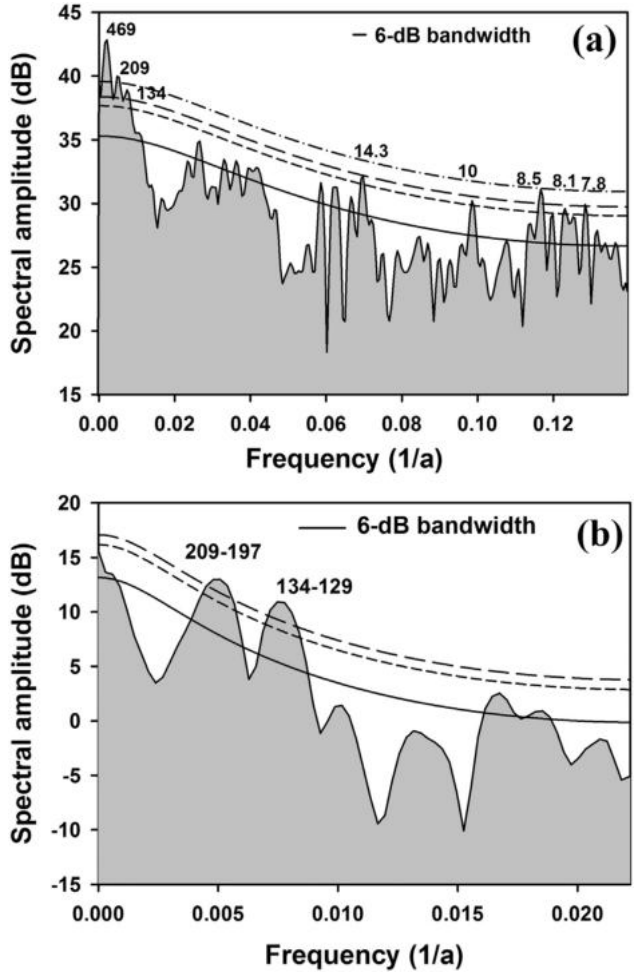

Fig. 9. Results of spectral analysis for (a) Pookot Lake sediment χ_{lf} data corresponding to the period −57 to 1117 cal. years B.P. (b) Total solar irradiance data (Steinhilber et al., 2012). REDFIT 3.8 software was used with Welch window and an over-sampling factor (OFAC) of 4.0. The number of segments that overlap one another by 50% is 4. Prominent periodicities are marked above the peaks. The solid line indicates the first order auto regressive curve. Short dashed and long dashed lines indicate 90% and 95% false alarm levels (χ^2) respectively.

numbers, there was good coherency for the 12.1, 8.1–7.5, 6.7 and 5.9 year periodicities. Agnihotri et al. (2002) carried out spectral analysis of the reconstructed TSI based on ^{10}Be and ^{14}C (Bard et al., 2000) as well as annual sunspot numbers (Lean et al., 1995). The former yielded periodicities of 210, 125 and 91 years and the latter 194, 113, 77 and 53 years. Spectral analysis of TSI data (Steinhilber et al., 2012; ftp://ftp.ncdc.noaa.gov/pub/data/paleo/climate_forcing/solar_variability/steinhilber2012.xls accessed on 14/03/2015) yielded periodicities of 209–197 and 134–129 years (Fig. 9b). Cross spectral analysis of PK χ_{lf} and TSI data (Steinhilber et al., 2012) indicates high coherency for the 418, 76 and 65 year periodicities (Fig. 10c). The shorter periodicities are not recorded may be because of the coarse resolution of TSI data.

Most of these periodicities appear similar to those modulated by the Sun (Supplementary Table S1). However, finding similar periodicities may not suggest a causal relationship between TSI and magnetic parameters. Phase analysis indicates that both the parameters are out of phase, with χ_{lf} leading TSI (Fig. 10d). This indicates that there is no causal relationship between the two, although their broad trends are similar. Therefore, we wish to suggest that solar minima and magnetic susceptibility are not aligned at the present state of knowledge.

3.6. Comparison with other palaeoclimatic records from the region

We compared the environmental magnetic record of Pookot Lake (PK) sediments (Fig. 11) with other continental and marine palaeoclimatic records from the region (Fig. 1a) to explore regional trends of rainfall during the past 3100 years.

A weak monsoon during the Little Ice Age and a strong monsoon during the Medieval Warm Period documented in the PK sediment record are also recorded in the organic carbon content of a sediment core from the eastern Arabian Sea (Agnihotri et al., 2002; Fig. 11a) and the δ^{18}O of *Globigerinoides ruber* from a sediment core off Mangalore coast (Tiwari et al., 2005; Fig. 11b). Both the records show low rainfall during LIA and high rainfall during MWP. The varve thickness record from a sediment core off Pakistan (von Rad et al., 1999; Fig. 10c) also exhibits a similar pattern, with an increased runoff from the Indus River recorded during 1000–700 cal. years B.P. and a decreased runoff during 700–400 cal. years B.P.

A conspicuous peak in rainfall is recorded around 300 cal. years B.P. (1650 AD) in the PK record (marked as 'H'). It may correspond to the high-rainfall period around 1666 AD (ER1) when the Akalagavi speleothem (Fig. 11d) started growing (Yadava et al., 2004). Bhattacharyya and Yadav (1999) also documented high ring width for a tree from western India for the same year. The magnetic susceptibility record of TK Lake in southern India also shows high values during 1640 AD, indicating high rainfall during this period (Shankar et al., 2006). The historically recorded droughts of 1777 AD and 1796 AD documented in the Akalagavi speleothem (as DR7 and DR8; Yadava et al., 2004) are seen as a trough in the PK χ_{lf} record around 200 cal. years B.P. (1750 AD) (marked as 'L').

The Dandak and Gupteshwar speleothems (Yadava and Ramesh, 2005) recorded high rainfall around 600 years B.P. (Fig. 11e and f). Reconstructed rainfall data using the Gupteshwar and Dandak speleothem records suggest low rainfall during LIA compared to MWP (Sinha et al., 2007; Yadava and Ramesh, 1999a, 1999b; Yadava and Ramesh, 2005).

The oxygen isotope profile of a speleothem (S3) from southern Oman (Fleitmann et al., 2004; Fig. 8g) recorded low rainfall between 1310 AD and 1660 AD. Fleitmann et al. (2004) suggested that the transition from the Medieval Warm Period to the Little Ice Age occurred approximately around 1310 AD based on a distinct shift to more positive δ^{18}O values, coinciding with a significant reduction in rainfall. The lowest rainfall is recorded between 1450 AD and 1480 AD. The Pookot Lake record has also documented this with a sharp decrease in magnetic parameter values around 1400 AD (~550 cal. years B.P.). There is no agreement on the duration of LIA; its termination has been placed variously at 1700, 1850 or even 1900 AD (Lamb, 1977). But rainfall exhibits an increasing trend after 1660 AD and is almost entirely above the long-term average in Oman (Fleitmann et al., 2004). The PK record shows an increasing trend of rainfall post-350 cal. years B.P. (1600 AD) and a constant rainfall post-200 cal. years B.P. (1750 AD). Hence, the Little Ice Age seems to be short-lived in the region as suggested by Fleitmann et al. (2004) and may be placed at 1400–1600 AD. The 1600–1750 cal. year B.P. period experienced low rainfall conditions compared to the present, although it displays an increasing trend. Hence, the termination of LIA may not be exactly around 1600 AD, but somewhere between 1600 and 1750 AD. Although there are short intervals of low rainfall after 1750 AD, the overall rainfall is high.

These high- and low-rainfall periods are also documented in the geochemical record of a sediment core from the southeastern Arabian Sea (Chauhan et al., 2010; Fig. 11h) off Kerala. The geochemical record suggests low rainfall around 1000 and 650–450 cal. years B.P. and high rainfall during 900–650 cal. years B.P. A sudden weakening of the monsoon around 950 cal. years B.P. is also documented in the PK record (which is a brief spell of low rainfall during MWP) after which there is an increasing trend. Post-400 cal. years B.P., an increasing trend in rainfall is recorded by all the proxies; this is documented in the PK record too around the same time (~350 cal. years B.P.).

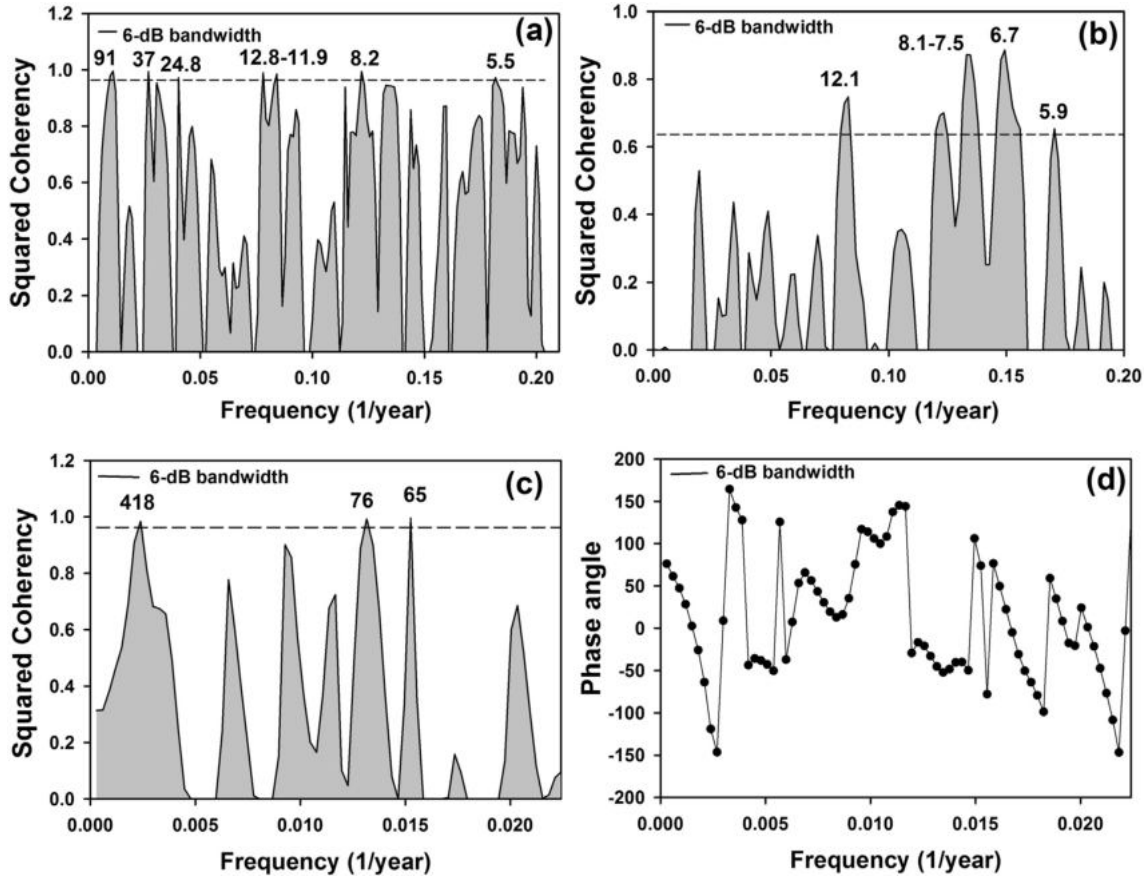

Fig. 10. Results of cross spectral analysis. (a) Coherency spectra for annual sunspot numbers (A.D. 1700 to 2007) and χ_{lf}; (b) Coherency spectra for group sunspot numbers (A.D. 1610 to 2005) and χ_{lf}; (c) Coherency spectra for TSI (Steinhilber et al., 2012) and χ_{lf} (for the past 1200 years); (d) Phase analysis of TSI (Steinhilber et al., 2012) and χ_{lf} (indicating that χ_{lf} leads TSI). Note: The horizontal broken line indicates 90% significance level. Periodicities are shown above the peaks.

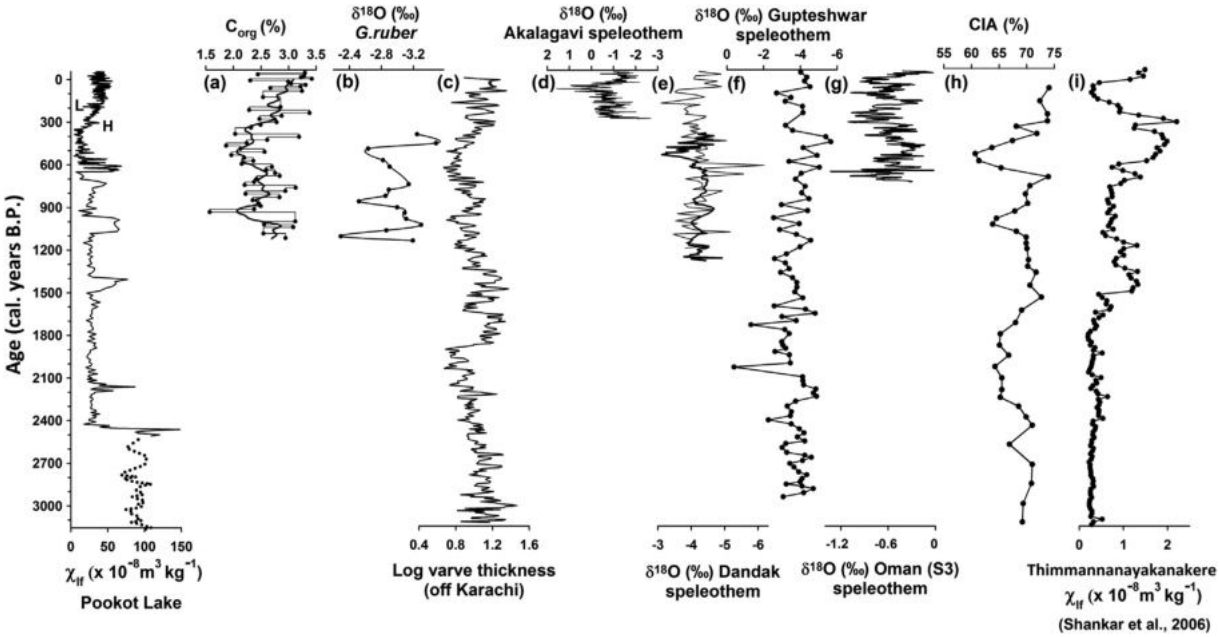

Fig. 11. Comparison of PK sediment χ_{lf} record (solid lines indicate data from core PK2 and dotted line data from core PK1) with other palaeoclimatic records from the region. (a) C_{org} record from an eastern Arabian Sea sediment core (Agnihotri et al., 2002); (b) $\delta^{18}O$ of *G. ruber* from an eastern Arabian Sea sediment core off Mangalore coast (Tiwari et al., 2005); (c) Varve thickness of sediments from the NE Arabian Sea off Karachi (von Rad et al., 1999, 2006); (d) $\delta^{18}O$ of Akalagavi speleothem (Yadava et al., 2004); (e & f) $\delta^{18}O$ of Dandak (thin line — Yadava and Ramesh, 2005; thick line — Sinha et al., 2007) and Gupteshwar speleothems (Yadava and Ramesh, 2005); (g) $\delta^{18}O$ of stalagmites (S3) from Oman (Fleitmann et al., 2004); (h) Geochemical record (chemical index of alteration) from a southeastern Arabian Sea sediment core (Chauhan et al., 2010); and (i) Sediment χ_{lf} record from Thimmannanayakanakere, Chitradurga, southern India (Shankar et al., 2006).

During 2400–1100 cal. years B.P., rainfall was steady and relatively low compared to the Present. An arid phase was recorded by Chauhan et al. (2010) during 2200–1800 cal. years B.P. and a wet phase subsequently up to 1100 cal. years B.P. But in the PK record, this arid phase is longer and interspersed by a few, high-rainfall intervals. Varve thickness data of von Rad et al. (1999, 2006) indicate precipitation minima during 2100–1900 and 1900–1400 cal. years B.P. Yadava and Ramesh (2005) documented an arid phase from 2000 to 1000 cal. years B.P. with two strong arid stints around 1700 and 2000 cal. years B.P. in the Gupteshwar speleothem record.

The wet phase documented in the PK record around 2400–3100 cal. years B.P. is concordant with the humid periods during 3000–2000 and 4000–2700 cal. years B.P. respectively recorded by Chauhan et al. (2010) and von Rad et al. (2006). Fleitmann et al. (2003) also documented a strong monsoon around 3000 cal. years B.P. based on the $\delta^{18}O$ record of a speleothem (Q5) from the Qunf Cave, southern Oman. But a long drought or weakening of the summer monsoon was documented in Rajasthan lakes (Lunkaransar and Didwana) between 3600 and 2000 cal. years B.P. (Bryson and Swain, 1981; Swain et al., 1983; Prasad et al., 1997). According to these records, the wet phase got terminated around 3500 cal. years B.P. and dry conditions like in the modern times persisted until around 2000 cal. years B.P. Chauhan et al. (2010) attributed this discordance to the archival efficiency of the proxies. As these lakes are located in a region of extremely high temperature and abysmally low rainfall, a marginal increase in precipitation may not alter the vegetation pattern or pollen flux; hence, a record from the southwest continental margin of India (which receives a much higher rainfall compared to the former) cannot be compared with a secondary vegetation response (Chauhan et al., 2010). Sarkar et al. (2000) attributed the aridity to the large spatial variability of the monsoon over the subcontinent and suggested that the *Sahyadri* (the Western Ghat) did not experience significant aridity around 4000 cal. years B.P. The $\delta^{18}O$ record of Gupteshwar speleothem (Yadava and Ramesh, 2005) displays high rainfall between 3400 and 2900 cal. years B.P., a gradual decrease subsequently and a comparatively low rainfall between 2900 and 1200 cal. years B.P. Varved sediments also show that the decrease in rainfall (after 2700 cal. years B.P.) was gradual, with the lowest rainfall documented around 2000 cal. years B.P. But in the PK record the shift from high to low rainfall conditions around 2400 cal. years B.P. is abrupt. As Pookot Lake is situated in a high-rainfall region (~4200 mm annual rainfall) and Rajasthan receives <500 mm annual rainfall, a comparison of their palaeoclimatic records is not reasonable. As per the TK lake record (Shankar et al., 2006; Fig. 11i), which is only about 400 km away from PK, dry conditions prevailed up to 1550 cal. years B.P., after which the monsoon began to strengthen and relatively high rainfall conditions persisted up to ~663 cal. years B.P. There are dissimilarities in the palaeorainfall records of the two lakes. Such dissimilarities between the χ_{lf} records of the two not-so-distant lakes point to regional variability of rainfall in the past. This is not surprising when the spatial variability of the modern rainfall is considered (Parthasarathy et al., 1993). This is because the two lakes experience entirely different climatic conditions at the present: TK being situated in a semi-arid area has an average annual rainfall of 638 mm whereas PK is situated in the *Sahyadri* (the Western Ghat) with an average annual rainfall of ~4200 mm.

4. Conclusions

Pookot Lake sediments have provided a palaeoenvironmental record of the region for the past 3100 cal. years. Pookot is one of the few lakes in southern India that have been investigated. Variations in the magnetic parameters reflect changes in the local environment that are linked probably to rainfall and/or changes in the water table. The rainfall-dependent catchment erosion (detrital influx) model may be applied here to explain the variations in magnetic parameters. The magnetite in the Pookot Lake sediments is mainly catchment-derived and rainfall is the most likely dominant driving mechanism behind variations in the magnetic properties of PK sediments. The detrital influx to the Pookot Lake, and hence rainfall in the Pookot catchment, has varied significantly during the past 3100 years. Noteworthy are the following features: (a) ~3100 to 2500 cal. years B.P.: Detrital influx and catchment erosion were very high, indicating a strong monsoon (the highest value of χ_{lf} in this section of the cores); (b) 2500 to 1000 cal. years B.P.: Low and steady rainfall interspersed with brief spells of strong monsoon as detrital influx and catchment erosion were uniform and low; (c) ~1000 cal. years B.P. to the Present: There was high catchment erosion indicating a shift to strong monsoonal conditions. Although the monsoon was generally strong during this period, there were short low-rainfall intervals in between.

The broad trends of total solar irradiance and χ_{lf} (=rainfall) are similar with periods of high TSI characterised by high rainfall (χ_{lf}) and vice versa. However, smaller variations in TSI and χ_{lf} are out of phase which we are unable to explain with the present state of knowledge although they may be due to age-depth uncertainties. Rainfall in the region was relatively low during the Little Ice Age and high during the Medieval Warm Period. This seems to be the overall trend of rainfall documented not only by Pookot Lake sediments but by other continental and marine palaeoclimatic records from a wider region of the Indian sub-continent. Rainfall in the region exhibits a number of periodicities with a prominent 10-year period.

Acknowledgements

SK thanks UGC (University Grants Commission), New Delhi, for financial assistance in the form of Junior and Senior Research Fellowships. AKW thanks the Council of Scientific and Industrial Research (CSIR), Government of India, for a senior research fellowship. The magnetic instruments used in this study were procured from grants made available by the erstwhile Department of Ocean Development (now Ministry of Earth Sciences), Government of India, through a research project (DOD/11-MRDF/1/48/P/94-ODII/12-10-96) to RS. We thank Dr. Jobish, Dr. Harshavardhana, B.G., M/s. Binu and Thomas for their assistance during field work and collection of cores. We thank Dr. Avinash Kumar for help in preparing the location map. We are grateful to Prof. Klaus Holliger (Editor) the two anonymous referees whose comments helped improve the final manuscript.

Appendix A. Supplementary data

Supplementary data to this article can be found online at http://dx.doi.org/10.1016/j.jappgeo.2015.03.023.

References

Agnihotri, R., Dutta, K., Bhushan, R., Somayajulu, B.L.K., 2002. Evidence for solar forcing on the Indian monsoon during the last millennium. Earth Planet. Sci. Lett. 198, 521–527.
Ananthapadmanabha, A.L. 2014. Mineral magnetic characterisation of soils of northern Kerala, India. Unpublished PhD thesis, Mangalore University, Mangalagangotri, India, 188 pp.
Ananthapadmanabha, A.L., Shankar, R., Sandeep, K., 2014a. Rock magnetic characterisation of tropical soils from southern India: implications to pedogenesis and soil erosion. Int. J. Environ. Res. 8 (3), 659–670.
Ananthapadmanabha, A.L., Shankar, R., Sandeep, K., 2014b. Rock magnetic properties of lateritic soil profiles from southern India: evidence for pedogenic processes. J. Appl. Geophys. 111, 203–210.
Anderson, N.J., Rippey, B., 1988. Diagenesis of magnetic minerals in the recent sediments of a eutrophic lake. Limnol. Oceanogr. 33, 1476–1492.
Bard, E., Raisbeck, G., Yiou, F., Jouzel, J., 2000. Solar irradiance during the last 1200 years based on cosmogenic nuclides. Tellus 52B, 985–992.
Bhattacharyya, A., Yadav, R.R., 1999. Climatic reconstruction using tree-ring data from tropical and temperate regions of India — a review. IAWA J. 20 (3), 311–316.
Bhattacharyya, A., Sandeep, K., Misra, S., Shankar, R., Warrier, A.K., Weijian, Z., Xuefeng, L., 2015. Vegetational and Climatic Variations during the Past 3100 years in Southern India: Evidence from Pollen, Magnetic Susceptibility and Particle Size data. Environ. Earth Sci. (under review).
Blaauw, M., 2010. Methods and code for 'classical' age-modelling of radiocarbon sequences. Quat. Geochronol. 5 (5), 512–518.

Blaha, U., Saptoka, B., Appel, E., Stanjek, H., Rosler, W., 2008. Micro-scale grain-size analysis and magnetic properties of coal-fired power plant fly ash and its relevance for environmental magnetic pollution studies. Atmos. Environ. 42, 8359–8370.
Bonnefille, R., Anupama, K., Barboni, D., Pascal, J.P., Prasad, S., Sutra, J.P., 1999. Modern pollen spectra from tropical South India and Sri Lanka. J. Biogeogr. 26, 1255–1280.
Bradak, B., Szakmany, G., Jozsa, S., Prichystal, A., 2009. Application of magnetic susceptibility on polished stone tools from Western Hungary and the Eastern part of the Czech Republic (Central Europe). J. Archaeol. Sci. 36, 2437–2444.
Bryson, R.A., Swain, A.M., 1981. Holocene variations in monsoon rainfall in Rajasthan. Quat. Res. 16, 135–145.
Chandran, P.P., 2003. District Handbooks of Kerala–Wayanad. In: Rajasekharan, G., Santhosh Kumar, K. (Eds.), Department of Information and Public relations, Govt. of Kerala.
Chauhan, O.S., Vogelsang, E., Basavaiah, N., Syed Abdul Kader, U., 2010. Reconstruction of the variability of the southwest monsoon during the past 3 ka from the continental margin of the southeastern Arabian Sea. J. Quat. Sci. 25, 798–807.
Damon, P.E., Peristykh, A.N., 2000. Radiocarbon calibration and application to geophysics, solar physics and astrophysics. Radiocarbon 42 (1), 137–150.
Dearing, J.A., 1999. Magnetic susceptibility. In: Walden, J., Smith, J.P., Oldfield, F. (Eds.), Environmental Magnetism — A Practical Guide. Technical Guide No 6. Quaternary Research Association, London, pp. 35–62.
Dearing, J.A., Elner, J.K., Happey-Wood, C.M., 1981. Recent sediment flux and erosional processes in a Welsh upland lake catchment based on magnetic susceptibility measurements. Quat. Res. 16, 356–372.
Dearing, J.A., Bird, P.M., Dann, R.J.L., Benjamin, S.F., 1997. Secondary ferromagnetic minerals in Welsh soils: a comparison of mineral magnetic detection methods and implications for mineral formation. Geophys. J. Int. 130, 727–736.
Eddy, J.A., 1976. The Maunder Minimum. Science 192, 1189–1202.
Fleitmann, D., Burns, S.J., Mudelsee, M., Neff, U., Kramers, J., Mangini, A., et al., 2003. Holocene forcing of the Indian monsoon recorded in a stalagmite from Southern Oman. Science 300, 1737–1739.
Fleitmann, D., Burns, S.J., Neff, U., Mudelsee, M., Mangini, A., Matter, A., 2004. Palaeoclimatic interpretation of high-resolution oxygen isotope profiles derived from annually laminated speleothems from Southern Oman. Quat. Sci. Rev. 23, 935–945.
Foster, I.D.L., Oldfield, F., Flower, R.J., Keatings, K., 2008. Mineral magnetic signatures in a long core from Lake Qarun, Middle Egypt. J. Paleolimnol. 40, 835–849.
Gautam, P., Blaha, U., Appel, E., Neupane, G., 2004. Environmental magnetic approach towards the quantification of pollution in Kathmandu urban area, Nepal. Phys. Chem. Earth 29, 973–984.
Geiss, C.E., Umbanhowar, C.E., Cammil, P., Banerjee, S.K., 2003. Sediment magnetic properties reveal Holocene climate change along Minnesota prairie-forest ecotone. J. Paleolimnol. 30, 151–166.
Geiss, C.E., Zanner, C.W., Banerjee, S.K., Minott, J., 2004. Signature of magnetic enhancement in a loessic soil in Nebraska, United States of America. Earth Planet. Sci. Lett. 228 (3–4), 355–367.
Geological and Mineral Map of Kerala 1995. Compiled by. Mallikarjuna, C., Nair, M.M., Gopalakrishnan, L.S., Adiga, K.S., Nambiar, A.R., Balakrishnan, P. et al., Geological Survey of India, scale 1. 500000, 1 sheet.
Hoyt, D.V., Schatten, K.H., 1997. Group sunspot numbers: a new solar activity reconstruction. Sol. Phys. 179, 189–219.
India Meteorological Department, 2008. Rainfall Data for Vythiri Station. Government of India, New Delhi.
Jelinowska, A., Tucholka, P., Wieckowski, K., 1997. Magnetic properties of sediments in a Polish lake: evidence of a relation between the rock-magnetic record and environmental changes in Late Pleistocene and Holocene sediments. Geophys. J. Int. 129, 727–736.
Juyal, N., Pant, R.K., Basavaiah, N., Bhushan, R., Jain, M., Saini, N.K., et al., 2009. Reconstruction of Last glacial to early Holocene monsoon variability from relict lake sediments of the Higher Central Himalaya, Uttarakhand, India. J. Asian Earth Sci. 34 (3), 437–449.
Kajale, M.D., Deotare, B.C., 1997. Late Quaternary environmental studies on salt lakes in western Rajasthan, India: a summarised view. J. Quat. Sci. 12 (5), 405–412.
Kerala Forest Department, 1986. Working Plan Report for the Kozhikode forest division. Department of Forests, Thiruvananthapuram, Government of Kerala.
Kotlia, B.S., Sharma, C., Bhalla, M.S., Rajagopalan, G., Subrahmanyam, K., Bhattacharyya, A., et al., 2000. Palaeoclimatic conditions in the late Pleistocene Wadda Lake, eastern Kumaun Himalaya, India. Palaeogeogr. Palaeoclimatol. Palaeoecol. 162, 105–118.
Krishnamurthy, R.V., Bhattacharya, S.K., Kusumgar, S., 1986. Palaeoclimatic changes deduced from $^{13}C/^{12}C$ and C/N ratios of Karewa lake sediments, India. Nature 323, 150–152.
Lamb, H.H. 1977. Climate: Present, Past and Future. vol 2: Climatic History and the Future. Methuen London Barnes and Noble, New York, 835 pp.
Lean, J., Beer, J., Bradley, R., 1995. Reconstruction of solar irradiance since 1610: implications for climate change. Geophys. Res. Lett. 22, 3195–3198.
Maher, B.A., 1988. Magnetic properties of some synthetic sub-micron magnetites. Geophys. J. R. Astron. Soc. 94, 83–96.
Maher, B.A., Taylor, R.M., 1988. Formation of ultrafine-grained magnetite in soils. Nature 336, 368–370.
Maher, B.A., Thompson, R., 1992. Palaeoclimatic significance of the mineral magnetic record of the Chinese loess and palaeosols. Quat. Res. 39, 155–170.
Maher, B.A., Thompson, R., 1995. Palaeorainfall reconstruction from pedogenic magnetic susceptibility variations in the Chinese loess and palaeosols. Quat. Res. 44, 383–391.
Maher, B.A., Alekseev, A., Alekseeva, T., 2003. Magnetic mineralogy of soils across the Russian Steppe: climatic dependence of pedogenic magnetite formation. Palaeogeogr. Palaeoclimatol. Palaeoecol. 201, 321–341.
Mighall, T.M., Foster, I.D.L., Crewd, P., Chapman, A.S., Finn, A., 2009. Using mineral magnetism to characterize iron working and to detect its evidence in peat bogs. J. Archaeol. Sci. 36, 130–139.
Oldfield, F., 1991. Environmental magnetism: a personal perspective. Quat. Sci. Rev. 10, 73–85.
Oldfield, F., 1994. Toward the discrimination of fine grained ferrimagnets by magnetic measurements in lake and near-shore marine sediments. J. Geophys. Res. 99, 9045–9050.
Oldfield, F., 1999. Introduction. In: Walden, J., Smith, J.P., Oldfield, F. (Eds.), Environmental Magnetism — A Practical Guide. Technical Guide No. 6. Quaternary Research Association, London, pp. 1–4.
Oldfield, F., 2007. Sources of fine grained magnetic minerals in sediments. A problem revisited. The Holocene 17 (8), 1265–1271.
Oldfield, F., Crowther, J., 2007. Establishing fire incidence in temperate soils using magnetic measurements. Palaeogeogr. Palaeoclimatol. Palaeoecol. 249, 362–369.
Oldfield, F., Hunt, A., Jones, M.D.H., Chester, R., Dearing, J.A., Olsson, L., Prospero, J.M., 1985. Magnetic differentiation of atmospheric dust. Nature 317, 516–518.
Oldfield, F., Battarbee, R.W., Boyle, J.F., Cameron, N.G., Davis, B., Evershed, R.P., et al., 2010. Terrestrial and aquatic ecosystem responses to late Holocene climate change recorded in the sediments of Lochan Uaine, Cairnorms, Scotland. Quat. Sci. Rev. 29, 1040–1054.
Parthasarathy, B., Rupa Kumar, K., Munot, A.A., 1993. Homogenous Indian Monsoon rainfall. Variability and prediction. J. Earth Syst. Sci. 102 (1), 121–155.
Peck, J.A., Green, R.R., Shanahan, T., King, J.W., Overpeck, J.T., Scholz, C.A., 2004. A magnetic mineral record of Late Quaternary tropical climate variability from Lake Bosumtwi, Ghana. Palaeogeogr. Palaeoclimatol. Palaeoecol. 215, 37–57.
Pozza, M.R., Boyce, J.I., Morris, W.A., 2004. Lake-based magnetic mapping of contaminated sediment distribution, Hamilton Harbour, Lake Ontario, Canada. J. Appl. Geophys. 57 (1), 23–41.
Prasad, S., Enzel, Y., 2006. Holocene palaeoclimates of India. Quat. Res. 66 (3), 442–453.
Prasad, S., Kusumgar, S., Gupta, S.K., 1997. A mid to late Holocene record of palaeoclimatic changes from Nal Sarovar: a palaeodesert margin lake in western India. J. Quat. Sci. 12 (2), 153–159.
R Development Core Team, 2010. R: A Language and Environment for Statistical Computing. R Foundation for Statistical Computing, Vienna Austria 3-900051-07-0 (http://www.R-project.org).
Reimer, P.J., Baillie, M.G.L., Bard, E., Bayliss, A., Beck, J.W., Blackwell, P.G., et al., 2009. IntCal09 and Marine09 radiocarbon age calibration curves 0–50000 years cal BP. Radiocarbon 51, 1111–1150.
Roberts, A.P., Turner, G.M., 1993. Diagenetic formation of ferromagnetic iron sulphide minerals in rapidly deposited marine sediments, South Island, New Zealand. Earth Planet. Sci. Lett. 115, 257–273.
Saini, H.S., Tandon, S.K., Mujtaba, S.A.I., Pant, N.C., 2005. Lake deposits of the northeastern margin of Thar Desert: Holocene (?) palaeoclimatic implications. Curr. Sci. 88 (12), 1994–2000.
Sandeep, K., Shankar, R., Krishnaswamy, J., 2011. Assessment of suspended particulate pollution in the Bhadra River catchment, southern India: an environmental magnetic approach. Environ. Earth Sci. 62, 625–637.
Sandeep, K., Warrier, A.K., Harshavardhana, B.G., Shankar, R., 2012. Rock magnetic investigations of surface and sub-surface soil samples from five lake catchments in tropical Southern India. Int. J. Environ. Res. 6 (1), 1–18.
Sarkar, A., Ramesh, R., Somayajulu, B.L.K., Agnihotri, R., Jull, A.J.T., Burr, G.S., 2000. High resolution Holocene monsoon record from the eastern Arabian Sea. Earth Planet. Sci. Lett. 177, 209–218.
Schulz, M., Mudelsee, M., 2002. REDFIT: estimating red-noise spectra directly from unevenly spaced palaeoclimatic time series. Comput. Geosci. 28, 421–426.
Schulz, M., Stattegger, K., 1997. Spectral analysis of unevenly spaced paleoclimatic time series. Comput. Geosci. 23, 929–945.
Shankar, R., Thompson, R., Galloway, R.B., 1994. Sediment source modelling: unmixing of artificial magnetization and natural radioactivity measurements. Earth Planet. Sci. Lett. 126, 411–420.
Shankar, R., Thompson, R., Prakash, T.N., 1996. Estimation of heavy and opaque mineral contents of beach and offshore placers using rock magnetic techniques. Geo-Mar. Lett. 16, 313–318.
Shankar, R., Prabhu, C.N., Warrier, A.K., Vijayakumar, G.T., Sekar, B., 2006. A multi-decadal rock magnetic record of monsoonal variations during the past 3700 years from a tropical Indian tank. J. Geol. Soc. India 68 (3), 447–459.
Shen, Z., Bloemendal, J., Barbara, M., Chiverrell, R.C., Dearing, J.A., Lang, A., Liu, Q., 2008. Holocene environmental reconstruction of sediment-source linkages at Crummock Water, English Lake District, based on magnetic measurements. The Holocene 18, 129–140.
Sinha, A., Cannariato, K.G., Stott, L.D., Cheng, H., Edwards, R.L., Yadava, M.G., et al., 2007. A 900-year 600 to 1500 AD record of the Indian summer monsoon precipitation from the core monsoon zone of India. Geophys. Res. Lett. 34, L16707. http://dx.doi.org/10.1029/2007GL030431.
Snowball, I.F., 1991. Magnetic hysteresis properties of greigite (Fe_3S_4) and a new occurrence in Holocene sediments from Swedish Lappland. Phys. Earth Planet. Int. 68, 32–40.
Snowball, I., Thompson, R., 1990. A stable chemical remanence in Holocene sediments. J. Geophys. Res. 95, 4471–4479.
Soman, K., 1997. Geology of Kerala. Geological Society of India, Bangalore (280 pp.).
Srivastava, P., Kumar, Anil, Mishra, A., Meena, A.K., Tripathi, J.K., Sundriyal, Y.P., Agnihotri, R., Gupta, A.K., 2013. Early Holocene monsoonal fluctuations in the Garhwal higher Himalaya as inferred from multi-proxy data from the Malari palaeolake. Quat. Res. 80, 447–458.
Steinhilber, F., Abreu, J.A., Beer, J., Brunner, I., Christl, M., Fischer, H., Heikkilä, U., Kubik, P.W., Mann, M., McCracken, K.G., Miller, H., Miyahara, H., Oerter, H., Wilhelms, F., 2012. 9,400 years of cosmic radiation and solar activity from ice cores and tree rings. Proc. Natl. Acad. Sci. U. S. A. 109 (16), 5967–5971.

Swain, A.M., Kutzbach, J.E., Hastenrath, S., 1983. Estimates of Holocene precipitation for Rajasthan, India based on pollen and lake level data. Quat. Res. 19, 1–17.
Thompson, R., Oldfield, F., 1986. Environmental Magnetism. Allen and Unwin, London (227 pp.).
Tiwari, M., Ramesh, R., Somayajulu, B.L.K., Jull, A.J.T., Burr, G.S., 2005. Solar control of southwest monsoon on centennial time scales. Curr. Sci. 89, 1583–1588.
von Rad, U., Schaaf, M., Michels, K.H., Schulz, H., Berger, W.H., Sirocko, F., 1999. A 5000-yr record of climate change in varved sediments from the oxygen minimum zone off Pakistan, Northeastern Arabian Sea. Quat. Res. 51, 39–53.
von Rad, U., Luckge, A., Berger, W.H., Rolinski, H.D., 2006. Annual to millennial monsoonal cyclicity recorded in Holocene varved sediments from the NE Arabian sea. J. Geol. Soc. India 68 (3), 353–368.
Walden, J., 1999a. Sample collection and preparation. In: Walden, J., Smith, J.P., Oldfield, F. (Eds.), Environmental Magnetism — A Practical Guide. Technical Guide No 6. Quaternary Research Association, London, pp. 26–34.
Walden, J., 1999b. Remanence measurements. In: Walden, J., Smith, J.P., Oldfield, F. (Eds.), Environmental Magnetism — A practical guide. Technical Guide No 6. Quaternary Research Association, London, pp. 63–88.
Wang, X.S., 2013. Assessment of heavy metal pollution in Xuzhou urban topsoils by magnetic susceptibility measurements. J. Appl. Geophys. 92, 76–83.
Warrier, A.K., Shankar, R., Manjunatha, B.R., Harshavardhana, B.G., 2014a. Mineral magnetism of atmospheric dust over southwest coast of India. Impact of anthropogenic activities and implications to public health. J. Appl. Geophys. 102, 1–9.
Warrier, A.K., Mahesh, B.S., Mohan, R., Shankar, R., Asthana, R., Ravindra, R., 2014b. Glacial–interglacial climatic variations at the Schirmacher Oasis, East Antarctica: the first report from environmental magnetism. Palaeogeogr. Palaeoclimatol. Palaeoecol. 412, 249–260.
Yadava, M.G., Ramesh, R., 1999a. Palaeomonsoon record of the last 3400 years from speleothems of tropical India. Gondwana Geol. Mag. 4, 141–156.
Yadava, M.G., Ramesh, R., 1999b. Speleothems — useful proxies for past monsoon rainfall. J. Sci. Ind. Res. 58, 339–348.
Yadava, M.G., Ramesh, R., 2005. Monsoon reconstruction from radiocarbon dated tropical Indian speleothems. The Holocene 15, 48–59.
Yadava, M.G., Ramesh, R., Pant, G.B., 2004. Past monsoon rainfall variations in peninsular India recorded in a 331-year-old speleothem. The Holocene 14 (4), 517–524.
Yu, L., Oldfield, F., 1989. A multivariate mixing model for identifying sediment source from magnetic measurements. Quat. Res. 32, 168–181.